

# Composit structures $Ba_{0.5}Sr_{0.5}Co_{1-x}Fe_xO_{3-z}$ , synthesized on the big solar furnace

M. S. Payzullakhanov\*, F. Ernazarov, O. Rajamatov, N. Karshieva, A. Holmatov

Institute of Materials Science of the Academy of Sciences of the Republic of Uzbekistan, Tashkent 100084, Uzbekistan

\* Corresponding author: M. S. Payzullakhanov, fayz@bk.ru

## ARTICLE INFO

Received: 20 July 2023  
Accepted: 16 August 2023  
Available online: 8 October 2023

doi: 10.59400/esc.v1i1.138

Copyright © 2023 Author(s).

Energy Storage and Conversion is published by Academic Publishing Pte. Ltd. This article is licensed under the Creative Commons Attribution License (CC BY 4.0).  
<http://creativecommons.org/licenses/by/4.0/>

**ABSTRACT:** Anion-deficient structures based on the composition  $Sr_{0.5}Ba_{0.5}Co_{1-x}Fe_xO_{3-z}$  synthesized from a melt in a solar furnace in a stream of concentrated solar radiation with a density of 100–200 W/cm<sup>2</sup> have been studied. Briquettes of the form of tablets based on a stoichiometric mixture of carbonates and oxides of the corresponding metals ( $SrCO_3 + BaCO_3 + Co_3O_4 + Fe_2O_3$ ) were melted on the focal spot of the big solar furnace. Drops of the melt flowed into the water, cooling at a rate of 10<sup>3</sup> deg/s. Drops of the melt flowed into the water, cooling at a rate of 10<sup>3</sup> deg/s. The castings were crushed to a fineness of 63 μm, dried at 400 °C, molded into tablets (samples) (20 mm in diameter and 10 mm high). Samples of the material were sintered in the temperature range of 1050 °C–1250 °C. The structure, water absorption, and degradation in a carbon dioxide medium were studied in the samples. The crystal lattice of the material had a perovskite structure with a unit cell parameter  $a = 4.04 \text{ \AA}$ . The material samples showed increasing water absorption with increasing sintering temperatures. There is also a dependence on the resistance of the material structure to the effects of carbon dioxide and water vapor on the sintering temperature. The observed values of structural parameters indicate that the material based on the perovskite  $Sr_{0.5}Ba_{0.5}Co_{1-x}Fe_xO_{3-z}$  structures can be used as a catalyst in the production of hydrogen and synthesis gas by reforming and methane oxidation. Preliminary experiments on obtaining synthesis gas showed that the perovskite structures of the composition are not inferior to phosphogypsum in terms of efficiency. However, the implementation of such approaches requires the development and creation of special equipment that makes it possible to control the flows of gases and water into the reaction chamber irradiated by a concentrated flux of high-density solar radiation.

**KEYWORDS:** synthesis from a melt; concentrated flow; hydrogen production; synthesis gas; perovskite catalytic structures

## 1. Introduction

In the fundamental triad “composition-structure-properties”, one can trace the manifestation of unique properties (high-temperature superconductivity, magnetoresistance, ferroelectricity, catalytic activity) of materials with the  $ABO_3$  perovskite structure<sup>[1-6]</sup>. Because of this, such materials are widely used in various promising areas<sup>[7-9]</sup>. For example, in obtaining synthesis gas<sup>[10,11]</sup>.

Anion-deficient  $ABO_{3-\delta}$  structures with transition metals in B positions (Mn, Fe, Co, Ni, and Cu) can be distinguished from the class of perovskites. A feature of such structures, for example,  $SrBaCo_{1-x}Fe_xO_{3-z}$ , is mixed oxygen-electronic conductivity, which makes it possible to use them as oxygen-reversible ( $ABO_{3-\delta} + 1/2\delta O_2 \leftrightarrow ABO_3$ ) electrode materials, replacing expensive platinum in solid oxide fuel cells (SOFC). Oxygen-permeable membranes, reducing the cost of producing synthesis gas and sorbents with 100% oxygen selectivity<sup>[12-16]</sup>. Interest in materials of this class is especially growing under the conditions of rapidly developing hydrogen energy<sup>[17,18]</sup>. However, this material interacts well with carbon dioxide and decomposes into carbonates and oxides, which limits its applicability<sup>[19]</sup>. Perovskites are used in solid-oxide fuel cells to convert chemical energy into electricity. At the same time, such devices have high efficiency (more than 80%) and very low emissions of harmful gases. with high efficiency, low emissions, and fuel flexibility. In addition, perovskites are successfully used in membrane reactors based on oxygen-conducting membranes (OTMs). Such devices combine separation and chemical reactions in one unit<sup>[20]</sup>.

It was shown in the study of Pan et al.<sup>[21]</sup> that oxygen-conducting materials based on phosphogypsum significantly increase the efficiency of producing hydrogen-enriched synthesis gas (72.51% was established) at a reaction temperature of about 1023 K.

In this work, the material of the perovskite structure of the composition  $Ba_{0.5}Sr_{0.5}Co_{1-x}Fe_xO_{3-z}$ , was studied. The purpose of the work was to show the possibility of synthesizing perovskite structures in a solar furnace.

## 2. Methodology of experiments

A concentrated flux of solar radiation through mirror concentrating systems is widely used for heating, processing, and melting a wide range of materials. For example, a large solar furnace (BSP) with a thermal power of 1 MW was recently used to extract metals from industrial waste<sup>[22]</sup>, hydrogen from water<sup>[23]</sup>. The technological capabilities of BSP were also used to synthesize high-temperature materials<sup>[24]</sup>.

From mixtures of iron and cobalt oxides with barium and strontium carbonates ( $BaCO_3 + SrCO_3 + Fe_2O_3 + Co_2O_3$ ) in a stoichiometric ratio after grinding (63  $\mu m$ ) and molding by semi-dry pressing (100 MPa), samples were made in the form of a cylinder  $\approx 20$  mm, which were installed on a water-cooled melting unit located on the focal plane of the solar furnace. A concentrated flux of solar radiation with a density of the order of  $Q = 150$  W/cm<sup>2</sup> was directed to the sample. This value of the flux density is according to Stefan Boltzmann's law.

$$T = \sqrt[4]{\frac{Q}{\varepsilon\sigma}}$$

where  $Q$  is the flux density of the concentrated flux of solar radiation, 250 W/cm<sup>2</sup>,  $\varepsilon$  is the emissivity, and  $\sigma = 5.67 \times 10^{-8}$  W/m<sup>2</sup>K is the Stefan Boltzmann constant, corresponds to the temperature of the heated body of 2200 K. At this temperature, the sample melts, and melt drops fall into the water and are cooled at a rate of 10<sup>3</sup> deg/s. Such cooling conditions made it possible to fix the high-temperature structural states of the material.

Drops of the melt, loaded into the water, cracked into small glass-like particles of arbitrary shape. The melt quenched into water was crushed to a fineness of 60  $\mu\text{m}$  and molded into cylinders 8 mm in diameter and 2 mm high. Cylindrical samples were sintered at different temperatures.

X-ray phase analysis of samples of the obtained materials was performed on a Panalytical Empyrean diffractometer with software in the Bragg-Brentano reflection geometry with  $\text{CuK}\alpha$  radiation ( $\lambda = 1.5418 \text{ \AA}$ ). Data was taken between  $10^\circ$  and  $64^\circ$  in  $0.5^\circ$  increments.

Studies of the morphology and microstructural features of the material samples were done by scanning electron microscopy (SEM).

Thermogravimetric (TG) curves were obtained on a TG50 instrument either running in air at a heating rate of  $10 \text{ }^\circ\text{C}/\text{min}$  using about 50 mg of sample.

The temperature coefficient of thermal expansion was measured on a cathetometer in the temperature range of 300–1250 K. The electrical resistance was measured by the four-contact method in the temperature range of 300–1300 K.

The relative density of the samples was determined as the ratio of the density of the material sample to  $4.87 \text{ g}/\text{cm}^3$ .

### 3. Results and discussion

We have studied perovskite structures  $\text{Ba}_{0.5}\text{Sr}_{0.5}\text{Co}_{0.8}\text{Fe}_{0.2}\text{O}_{3-\delta}$  synthesized from a melt in a solar furnace.

**Figure 1** shows a Panalytical Empyrean X-ray diffractometer with  $\text{CuK}\alpha$  radiation of a sintered sample at  $1100 \text{ }^\circ\text{C}$ .

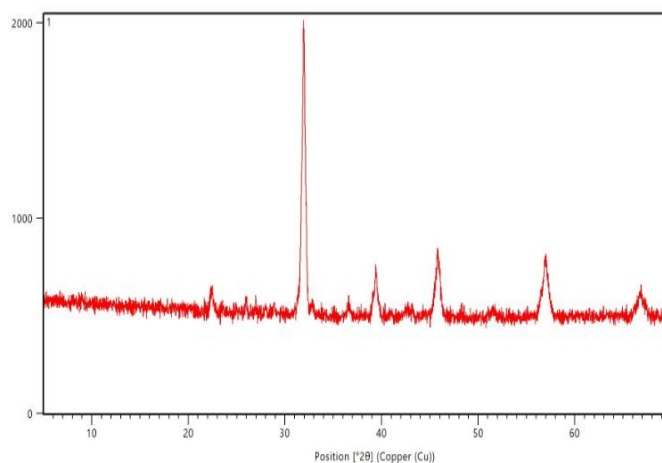


**Figure 1.** X-ray pattern of a material sample obtained by synthesis from a melt in a solar furnace of composition  $\text{Sr}_{0.5}\text{Ba}_{0.5}\text{Co}_{0.8}\text{Fe}_{0.2}\text{O}_{2.78}$ .

An analysis of the X-ray diffraction patterns showed that the obtained oxides have a cubic perovskite-like structure with a lattice parameter  $a = 4.04 \text{ \AA}$  of the  $\text{Pm}3\text{m}$  space group. It was also found that such structures are characterized by significant nonstoichiometry in oxygen. The estimated region of homogeneity of the resulting complex compositions of  $\text{Sr}_{0.5}\text{Ba}_{0.5}\text{Fe}_{1-x}\text{Co}_x\text{O}_{3-\delta}$  lies in the range from  $x = 0.0$  to  $x = 0.7$ .

**Figure 2** shows the dependence of shrinkage on the sintering temperature, and **Figure 3** shows the dependence of density on the sintering temperature.

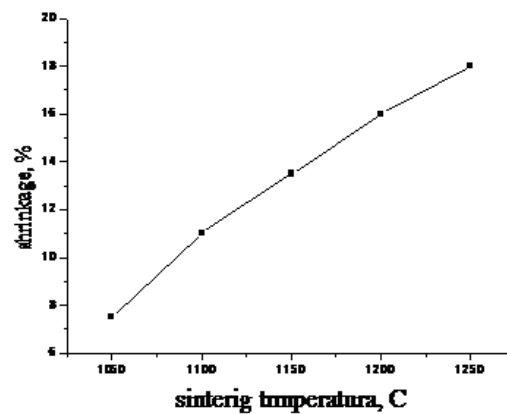


Figure 2. Dependence of shrinkage on sintering temperature.

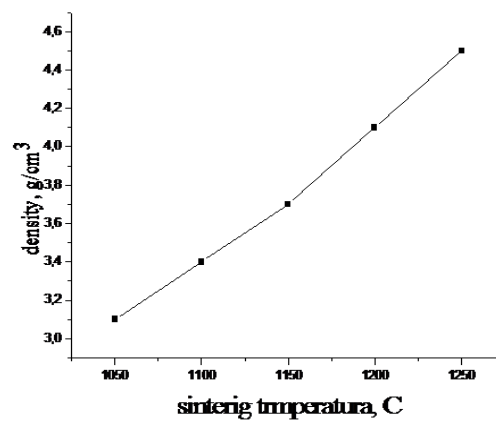


Figure 3. Dependence of density on sintering temperature.

As can be seen from **Figures 2 and 3**, with an increase in the sintering temperature of ceramics, an increase in shrinkage and density is observed. At the same time, a decrease in the porosity of the material is observed.

**Figure 4** shows the dependence of electrical resistance on the sintering temperature of material samples. As can be seen in **Figure 4**, with increasing temperature, an increase in electrical resistance is observed, i.e., samples of the material show a metallic character of conductivity.

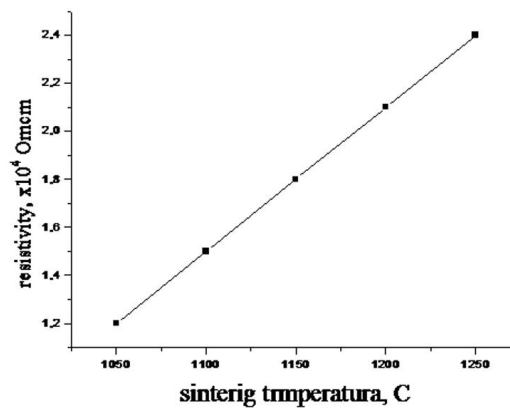


Figure 4. Dependence of electrical resistance on sintering temperature.

**Figure 5** shows the dependence of the water absorption of the material sample on the sintering temperature. As can be seen from **Figure 5**, an increase in the ceramic sintering temperature to 1200 °C

causes a decrease in water absorption. Thus, by the method of synthesis from a melt in a solar furnace, it is possible to obtain a material resistant to carbon dioxide and water vapor with low water absorption.

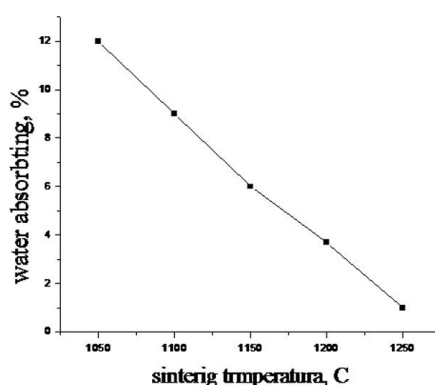
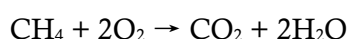
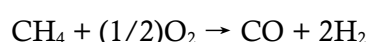
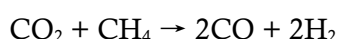
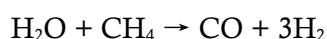


Figure 5. Dependence of water absorption on sintering temperature.

From the above, we can conclude that the material based on  $\text{Sr}_{0.5}\text{Ba}_{0.5}\text{Co}_{0.8}\text{Fe}_{0.2}\text{O}_{2.78}$  perovskite structures can be used as a catalyst in the production of hydrogen and synthesis gas by reforming and oxidizing methane:



Preliminary experiments on obtaining synthesis gas showed that the perovskite structures of the composition are not inferior to phosphogypsum in terms of efficiency.

However, the implementation of such approaches requires the development and creation of special equipment that makes it possible to control the flows of gases and water into the reaction chamber irradiated by a concentrated flux of high-density solar radiation.

## 4. Conclusion

Perovskite structures  $\text{Sr}_{0.5}\text{Ba}_{0.5}\text{Co}_{1-x}\text{Fe}_x\text{O}_{3-z}$  were synthesized from a melt in a solar furnace in a stream of concentrated solar radiation with a density of 100–200 W/cm<sup>2</sup>.

The material had a cubic structure with a unit cell parameter  $a = 4.04 \text{ \AA}$  and showed resistance to carbon dioxide and water vapor and low water absorption.

The material can be used as a catalyst in the production of hydrogen and synthesis gas by reforming and oxidizing methane.

## Author contributions

Conceptualization, MSP; methodology MSP; software, FE and OR; validation, FE, OR, NK and AH; supervision, MSP; project administration, MSP. All authors have read and agreed to the published version of the manuscript.

## Funding

The work was carried out within the framework of international projects AL-4821023123 “Technology of hydrogen storage in an absorbed form in porous materials” and IL-4821091562

“Peculiarities of phase transitions in ceramics synthesized using a solar furnace of the Institute of Materials Science of the Academy of Sciences of the Republic of Uzbekistan”.

## Conflict of interest

The authors declare no conflict of interest.

## References

1. Galasso FS. Structure, Properties and Preparation of Perovskite-Type Compounds. Pergamon Press; 1968.
2. Goodenough JB. Electronic and ionic transport properties and other physical aspects of perovskites. Reports on Progress in Physics. 2004, 67(11): 1915-1993. doi: 10.1088/0034-4885/67/11/R01
3. Peña MA, Fierro JLG. Chemical structures and performances of perovskite oxides. Chemical Reviews. 2001, 7(101): 1981-2017. doi: 10.1021/cr980129f
4. Yang JB, Kim J, Woo YS, et al. Magnetoresistance in double perovskites  $Ba_{2-x}La_xFeMoO_6$ . Journal of Magnetism and Magnetic Materials. 2007, 310(2): e664-e665. doi: 10.1016/j.jmmm.2006.10.916
5. Burns G, Dacol FH. Glassy polarization behavior in ferroelectric compounds  $Pb(Mg_{\{1\}/\{3\}}Nb_{\{2\}/\{3\}})O_3$  and  $Pb(Zn_{\{1\}/\{3\}}Nb_{\{2\}/\{3\}})O_3$ . Solid State Communications. 1983, 48(10): 853-856. doi: 10.1016/0038-1098(83)90132-1
6. Kharton VV, Patrakeev MV, Waerenborgh JC, et al. Methane oxidation over perovskite-related ferrites: Effects of oxygen nonstoichiometry. Solid State Sciences. 2005, 7(11): 1344-1352. doi: 10.1016/j.solidstatesciences.2005.08.004
7. Sharma S, Tomar M, Kumar A, et al. Photovoltaic effect in  $BiFeO_3/BaTiO_3$  multilayer structure fabricated by chemical solution deposition technique. Journal of Physics and Chemistry. 2016, 93: 63-67. doi: 10.1016/j.jpccs.2016.02.010
8. Zhang J, Gao X, Deng Y, et al. Comparison of life cycle environmental impacts of different perovskite solar cell systems. Solar Energy Materials and Solar Cells. 2017, 166: 9-17. doi: 10.1016/j.solmat.2017.03.008
9. Vassilakopoulou A, Papadatos D, Koutselas I. Light emitting diodes based on blends of quasi-2D lead halide perovskites stabilized within mesoporous silica matrix. Microporous and Mesoporous Materials. 2017, 249: 165-175. doi: 10.1016/j.micromeso.2017.05.001
10. Arutyunov VS. Oxidative Conversion of Natural Gas (Turkish). Krasand; 2011.
11. da Rosa AV, Ordóñez JC. Fundamentals of Renewable Energy Processes, 4th ed. Elsevier; 2022. pp. 419-470.
12. Bouwmeester HJM, Burggraf AJ. Dense ceramic membranes for oxygen separation. In: Gellings PJ, Bouwmeester HJM (editors). Handbook of Solid State Electrochemistry, 1st ed. CRC Press; 1997. pp. 481-553.
13. Tang M, Xu L, Fan M. Progress in oxygen carrier development of methane-based chemical-looping reforming: A review. Applied Energy. 2015, 151: 143-156. doi: 10.1016/j.apenergy.2015.04.017
14. Teraoka Y, Zhang H, Furukawa S, Yamazoe N. Oxygen permeation through perovskite-type oxides. Chemistry Letters. 1985, 14(11): 1743-1746. doi: 10.1246/cl.1985.1743
15. Shao Z, Yang W, Cong Y, et al. Investigation of the permeation behavior and stability of a  $Ba_{0.5}Sr_{0.5}Co_{0.8}Fe_{0.2}O_{3-\delta}$  oxygen membrane. Journal of Membrane Science. 2000, 172(1-2): 177-188. doi: 10.1016/S0376-7388(00)00337-9
16. Chang X, Zhang C, He Y, et al. A comparative study of the performance of symmetric and asymmetric mixed-conducting membranes. Chinese Journal of Chemical Engineering. 2009, 17(4): 562-570. doi: 10.1016/S1004-9541(08)60245-1
17. Payzullakhanov MS, Parpiev OR, Avezova NR, Shermatov Z. Hydrogen storage in porous ceramic materials of aluminosilicate composition. Applied Solar Energy. 2022, 58(5): 722-724. doi: 10.3103/S0003701X22601338
18. Allaev KR, Avezova NR. Hydrogen—The future of power engineering for the world and Uzbekistan. Applied Solar Energy. 2021, 57: 575-583. doi: 10.3103/S0003701X21060025
19. Zeng Q, Zuo Y, Fan C, Chen C.  $CO_2$ -tolerant oxygen separation membranes targeting  $CO_2$  capture application. Journal of Membrane Science. 2009, 335(1-2): 140-144. doi: 10.1016/j.memsci.2009.03.012
20. Sunarso J, Hashim SS, Zhu N, Zhou W. Perovskite oxides applications in high temperature oxygen separation, solid oxide fuel cell and membrane reactor: A review. Progress in Energy and Combustion Science. 2017, 61: 57-77. doi: 10.1016/j.peccs.2017.03.003

21. Pan Q, Ma L, Du W, et al. Hydrogen-enriched syngas production by lignite chemical looping gasification with composite oxygen carriers of phosphogypsum and steel slag. *Energy*. 2022, 241: 122927. doi: 10.1016/j.energy.2021.122927
22. Paizullakhanov MS, Parpiev OR, Yu RY, Suvanova SL. Features of the extraction of metals from waste in a solar furnace. *Applied Solar Energy*. 2022, 58(3): 433-437. doi: 10.3103/S0003701X2203015X
23. Akhatova JS, Ahmadova KS. Extraction of hydrogen from water using CeO<sub>2</sub> in a solar reactor using a concentrated flux of solar radiation. *Applied Solar Energy*. 2022, 58(6): 889-894. doi: 10.3103/S0003701X22060032
24. Paizullakhanov MS, Shermatov ZZ, Nodirmatov EZ, et al. Synthesis of materials by concentrated solar radiation. *High Temperature Material Processes*. 2021, 25(2): 17-29. doi: 10.1615/HighTempMatProc.2021038543